

RESEARCH ARTICLE

Zinc deficiency causes neural tube defects through attenuation of p53 ubiquitylation

Huili Li^{1,2}, Jing Zhang^{1,2} and Lee Niswander^{1,2,*}

ABSTRACT

Micronutrition is essential for neural tube closure, and zinc deficiency is associated with human neural tube defects. Here, we modeled zinc deficiency in mouse embryos, and used live imaging and molecular studies to determine how zinc deficiency affects neural tube closure. Embryos cultured with the zinc chelator TPEN failed to close the neural tube and showed excess apoptosis. TPEN-induced p53 protein stabilization *in vivo* and in neuroepithelial cell cultures and apoptosis was dependent on p53. Mechanistically, zinc deficiency resulted in disrupted interaction between p53 and the zinc-dependent E3 ubiquitin ligase Mdm2, and greatly reduced p53 ubiquitylation. Overexpression of human CHIP, a zinc-independent E3 ubiquitin ligase that targets p53, relieved TPEN-induced p53 stabilization and reduced apoptosis. Expression of p53 pro-apoptotic target genes was upregulated by zinc deficiency. Correspondingly, embryos cultured with p53 transcriptional activity inhibitor pifithrin- α could overcome TPEN-induced apoptosis and failure of neural tube closure. Our studies indicate that zinc deficiency disrupts neural tube closure through decreased p53 ubiquitylation, increased p53 stabilization and excess apoptosis.

KEY WORDS: Neural tube defect, Neural tube closure, Zinc deficiency, p53, Ubiquitylation, Live imaging

INTRODUCTION

Environmental factors influence neural tube closure (Wilde et al., 2014), and failure of closure leads to neural tube defects (NTDs), which are the second-most common birth defect worldwide. NTDs can occur in the cranial region (anencephaly, encephalocele), spinal region (spina bifida) or in combination (craniorachischisis or complex phenotypes) (Copp et al., 2013; Wallingford et al., 2013). Evidence from both experimental and epidemiological studies shows that lower folic acid concentrations are associated with human NTDs and that folic acid or inositol supplementation can reduce the risk of NTDs (Force et al., 2017; Greene et al., 2016; Jin, 2017; Viswanathan et al., 2017; Wilde et al., 2014). Neural tube closure is dependent on the methionine cycle and folate cycle (Leung et al., 2017). Other nutritional factors, such as trace elements, also influence the incidence of NTDs but their function relative to neural tube closure is less known (Copp et al., 2015).

Zinc is an essential trace element from microorganisms to human. Approximately 2800 human proteins can potentially bind zinc


in vivo through interactive regions such as zinc-finger motifs, including transcription factors and RING finger domain proteins that play a key role in the ubiquitylation pathway (Andreini et al., 2006). Wild-type female mice and rats fed a zinc-deficient diet yield embryos with NTDs: 4.4% of mouse embryos show exencephaly (Dufner-Beattie et al., 2006) and 3% of rats show spina bifida (Hurley, 1969). Zinc is ingested in food and absorbed into the body via several intestinal zinc transporters. Once absorbed, zinc enters the bloodstream, is taken up into cells and is further distributed to intracellular organelles. Zinc homeostasis is tightly controlled by zinc transporters and metallothioneins. Zinc transporters are divided into two major families: SLC39s/ZIPs, which take zinc into the cells; and SLC30s/ZnTs, which efflux zinc out of cells (Hojyo and Fukada, 2016). Homozygous *Zip1*^{-/-} (*Slc39a1*^{-/-}) and *Zip1*^{-/-}/*Zip3*^{-/-} (*Slc39a3*^{-/-}) mice fed a zinc-adequate diet (50 ppm zinc/day) show normal reproduction, and embryonic and neonatal growth rates. However, when dams were fed a severely zinc-deficient diet (<1 ppm zinc) beginning on embryonic day (E)8, 16% embryos with parental *Zip1* knockout and 54% embryos with parental *Zip1/Zip3* double knockout exhibit exencephaly at E14 (Dufner-Beattie et al., 2006). Transport of maternal zinc into the embryonic environment is mediated in part by ZNT1 and knockout of the *Znt1* (*Slc30a1*) gene causes early embryonic lethality (Andrews et al., 2004). These data highlight the association of zinc deficiency with embryonic development and NTDs, but the mechanism by which zinc deficiency affects neural tube closure is unclear.

Epidemiological reports in about 35 papers describe the status of zinc concentration in some human NTD cohorts (Fig. S1). The epidemiology data highlight that lower zinc levels in maternal or fetal tissues are associated with NTDs in Turkey (Çavdar et al., 1991, 1988; Cengiz et al., 2004; Demir et al., 2017; Zeyrek et al., 2009), Iran (Golalipour et al., 2009), China (Yan et al., 2017), Netherlands (Groenen et al., 2003), England (Buamah et al., 1984; Hinks et al., 1989; Leger et al., 1980), Bangladesh (Dey et al., 2010), Mexico (Carrillo-Ponce Mde et al., 2004) and India (Srinivas et al., 2001) (blue frames in Fig. S1). On the other hand, high levels of zinc accumulation are also associated with NTDs (red frames in Fig. S1), suggesting that the balance in zinc levels is important. Moreover, it has been suggested that higher peripheral zinc levels in some NTD cases may be a consequence of a deficiency of zinc uptake, ultimately resulting in zinc deficiency in the disease location. An experimental study has demonstrated that cultured skin fibroblasts from NTD cases with anencephaly and spina bifida show characteristics of decreased zinc uptake (Zimmerman and Rowe, 1983). Importantly, zinc-only or zinc-containing multiple micronutrient supplementation can decrease the risk of NTDs in humans (Czeizel, 1993; Czeizel and Dudas, 1992; Czeizel et al., 1994; Velie et al., 1999). Together, it appears that zinc deficiency has a causative role in some human NTD cases.

This evidence provided the impetus for the experimental studies reported here to explore how zinc deficiency impacts neural tube

¹Department of Pediatrics, University of Colorado Anschutz Medical Campus, Children's Hospital Colorado, Aurora, CO 80045, USA. ²Department of Molecular, Cellular and Development Biology, University of Colorado Boulder, Boulder, CO 80309, USA.

*Author for correspondence (lee.niswander@colorado.edu)

 H.L., 0000-0002-9248-0720; L.N., 0000-0002-9959-0594

closure. We have used mouse embryos and primary neuroepithelial cells cultured under zinc-deficient conditions to assess the effect of zinc deficiency on neural tube closure. Time-lapse live imaging methods and molecular studies demonstrate excess apoptosis in embryos during the process of neural tube closure. Moreover, we linked zinc deficiency with the attenuation of p53 ubiquitylation through the zinc-binding protein Mdm2, leading to p53 stabilization and abnormal apoptosis.

RESULTS

Zinc deficiency leads to failure of neural tube closure

To determine the effect of zinc deficiency on neural tube closure, we took advantage of a method to culture mouse embryos *ex utero*, which allows dynamic visualization of the process of neural tube closure (Massarwa and Niswander, 2013) and a means with which to induce intracellular zinc deficiency using TPEN, a membrane-permeable zinc ion chelator (Cho et al., 2007). The mouse embryo represents an excellent model for human neurulation, as shown by a similar closure process, similar NTD phenotypes and the findings that mouse genes discovered for their role in neural tube closure are correlated with deleterious variants in human NTD cases (Cai and Shi, 2014; Copp et al., 2013; Greene et al., 2009; Li et al., 2018; Wallingford et al., 2013). We used somite-matched E8.5 wild-type mouse embryos, which are just beginning to undergo neural tube closure and which carry a transgene that labels the cellular membranes with myristoylated Venus fluorescent protein (Ven^{Myr}) for time-lapse live imaging. Using 9-somite embryos at the start of the experiment, 100% of embryos cultured in control media closed the neural tube, and closure occurred by 9 h 18 min ± 1 h 37 min ($n=5$; Fig. 1A, Movie 1). In contrast, 100% of embryos at 9 somites treated with 15 μ M TPEN (at the lower level of previous studies that used a range of 1–100 μ M for cells) (Gao et al., 2017; Rayman et al., 2018; Strand et al., 2013) failed to close the neural tube; there was also a reduction in size of the cranial region and yolk sac, and there appeared to be an abundance of dead tissue in the midbrain-hindbrain region (Fig. 1C, Movie 2, Fig. S2). All of these TPEN-induced defects could be mitigated by the addition of 25 μ M ZnSO₄, as 100% of embryos treated with TPEN and ZnSO₄ closed their neural tube (Fig. 1D, Movie 3), although neural tube closure was delayed to 14 h 48 min ± 3 h 33 min ($n=6$). At a lower dose of TPEN (10 μ M), the neural tube closed (Fig. 1B) but cellular phenotypes were observed, as discussed below. This culture method provides a platform for our subsequent studies to determine the cellular and molecular basis for zinc deficiency-induced NTDs.

Zinc deficiency disrupts inflection of the neural folds

To explore further the effect of zinc deficiency on the process of neural tube closure, we quantified various morphogenetic parameters using still images from time-lapse movies. Cranial neural tube closure requires inflection and zippering of the neural folds (Massarwa and Niswander, 2013); therefore, we first examined the potential impact of zinc deficiency on these two morphological processes. Inflection was assessed by measurement of three parameters: perpendicular distance between neural folds, angle of the neural folds and distance between the approaching neural folds (Fig. 1E–G). Zippering was assessed using two parameters: rostral-caudal distance of closing neural folds and caudal zipper point angle (Galea et al., 2017) (Fig. 1H,I). Given that the neural folds in 15 μ M TPEN-treated embryos become obscure at around 7 h, we terminated the data collection of this treatment group at 7 h. In control, 10 μ M TPEN- and 15 μ M TPEN+ZnSO₄-treated embryos, inflection and zippering data points steadily decrease over

time (reflecting closure), although the time course is delayed for the TPEN+ZnSO₄ embryos. In contrast, inflection measurements in 15 μ M TPEN treatment showed an accelerated narrowing of the neural folds followed by a significant widening of the distance between the folds (Fig. 1E–G). These data demonstrate that zinc deficiency alters inflection. There was a relatively weak effect of zinc deficiency on zippering from the caudal zipper point (Fig. 1H), but the caudal zipper point angle changed approximately coincident with the alteration in inflection (Fig. 1I). One obvious feature of the 15 μ M TPEN-treated embryos is the reduction in the brain size and this was mitigated by the addition of zinc (Fig. 1C,D,J). Taken together, the major effect of TPEN-induced zinc deficiency is an alteration in neural fold inflection and reduced brain size.

Zinc deficiency causes excessive apoptosis during neural tube closure

The time-lapse videos of 15 μ M TPEN-treated embryos show significant amounts of apparently dead tissue coming out from the open neural tube and the rostral-caudal size of the brain is significantly reduced 6 h after TPEN treatment. This suggests abnormal apoptosis as the major cause of the zinc deficiency-induced NTD at the cellular level. Using the lower concentration of TPEN (10 μ M) and a shorter culture time (30 min and 2–4 h), we observed increased TUNEL-positive and cleaved caspase 3 (Casp3)-positive cells in the cranial regions of 6- to 10-somite stage embryos at the start of culture (Fig. 2A,B), and this could be suppressed by addition of zinc (Fig. 2C). The predominant tissue showing cleaved-Casp3 immunofluorescent staining was the neural ectoderm, with lesser and later staining in the non-neural ectoderm and even less in other regions, suggesting that the neuroectoderm is more sensitive to zinc deficiency than other cranial regions (Fig. 2A–C, Fig. S3). To determine whether a change in cell proliferation was also a contributor to the NTD, we assessed cell proliferation using phospho-histone H3 (pH3) staining and western blot analysis of 10 μ M and 15 μ M TPEN-treated E8.5 embryos. No changes were detected in the brain tissue (Fig. S4A,C). The lack of an observable change in cell proliferation, combined with the evidence that the cell cycle in the cranial neural tube is >12 h (Cameron and Greulich, 1963; Kim et al., 2007), suggests that the reduction in brain size and the NTD phenotype following TPEN treatment is due to excessive apoptosis. To evaluate the effect of zinc deficiency further, we turned to primary neuroepithelial cells isolated from E9.5 mouse brain. Consistent with the embryo results, TPEN treatment of neuroepithelial cells significantly increased the number of cleaved Casp3- and TUNEL-positive cells and zinc addition mitigated the TPEN-induced apoptosis phenotype, as shown by immunofluorescent staining and western blot analysis of cleaved Casp3 (Fig. 2D–F). This indicates that a major effect of zinc deficiency is excessive apoptosis during neural tube closure.

p53 plays a crucial role in zinc deficiency-induced excess apoptosis

The *Trp53* gene encodes the protein p53, a master regulator of cell survival. Increased levels of p53 initiate apoptosis, and p53 stability and activity are regulated by post-translational modifications and protein partner interactions. To determine whether zinc deficiency affects p53 levels, we treated E9.5 embryos for 3 h with TPEN and found that both cytoplasmic and nuclear levels of p53 in the brain region were dramatically increased; this induction was not observed upon culture with TPEN+ZnSO₄ (Fig. 3A). Similar results were found for primary E9.5 neuroepithelial cells (Fig. 3B).

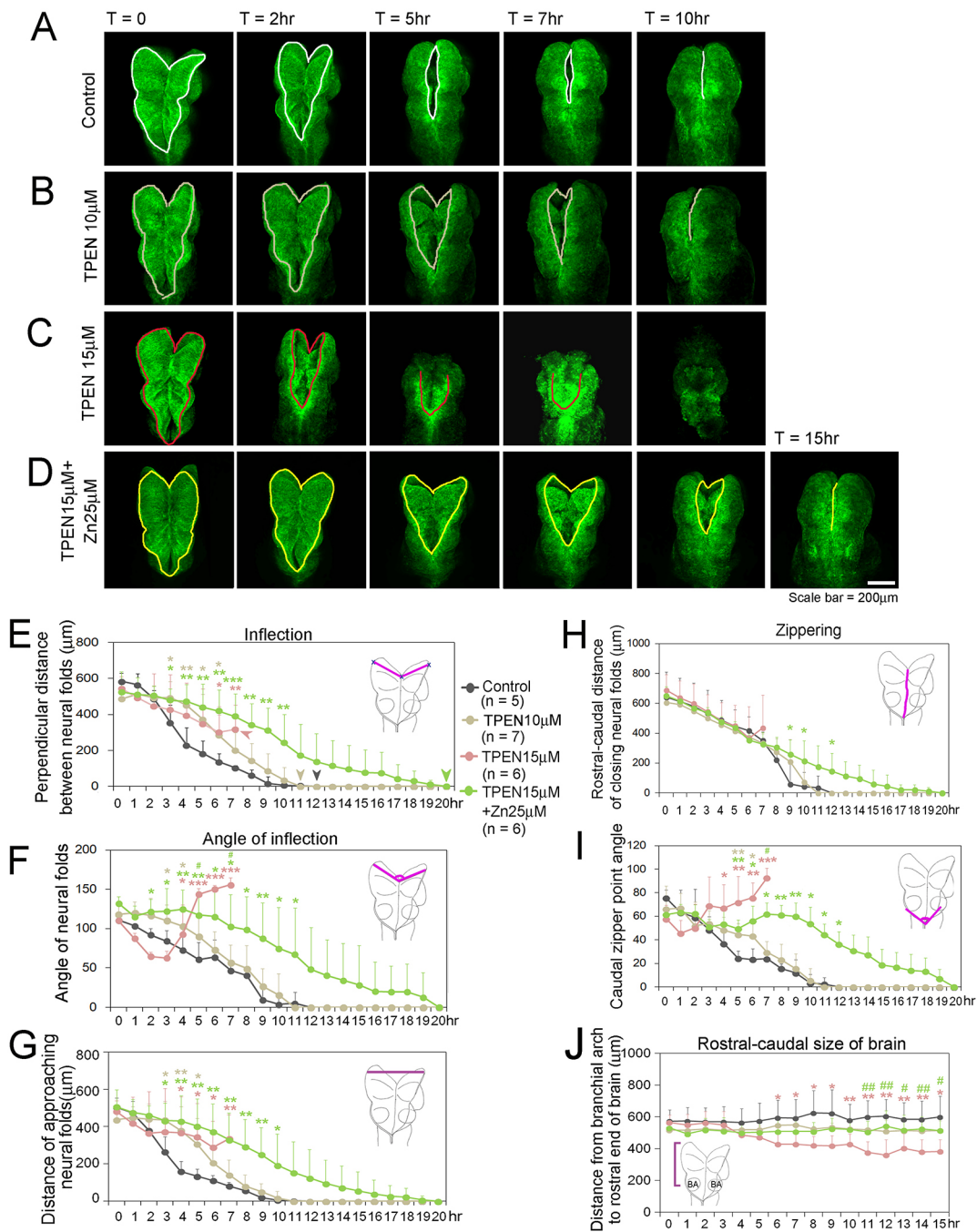


Fig. 1. Zinc deficiency disrupts the process of neural tube closure. (A-D) Typical still frames from time-lapse live imaging of E8.5 Ven^{Myr} mouse embryos. Embryos with 9 somites at the start of culture were grown overnight in control media (A, $n=5$ from four independent experiments) or media containing 10 μM TPEN (B, $n=7$ from four independent experiments), 15 μM TPEN (C, $n=6$ from three independent experiments) or 15 μM TPEN+25 μM ZnSO₄ (D, $n=6$ from two independent experiments). Dorsal views of midbrain and hindbrain regions. White, beige, red and yellow lines show the edges of neural folds. Scale bar: 200 μm . (E-J) Quantitative analysis of time-lapse live imaging. Inflection of the neural folds toward the midline is represented by the perpendicular distance between neural folds (E), the angle of neural folds (F) and the distance of approaching neural folds (G). Zippering in the hindbrain-midbrain region is represented by the rostral-caudal distance of closing neural folds (H) and the angle at caudal zipper point (I). The rostral-caudal size of the brain is inferred by rostral-caudal distance from branchial arch to rostral end of brain (J). Purple lines in cartoons display the positions of measurements. In E, the pink arrowhead indicates failure of neural tube closure; the dark gray, beige and green arrowheads indicate the timepoint of neural tube closure. * $P<0.05$ (TPEN10 μM versus control); * $P<0.05$ (TPEN15 μM versus control); * $P<0.05$ (TPEN15 μM +Zn versus control); # $P<0.05$ (TPEN15 μM +Zn versus TPEN15 μM). * $P<0.05$, # $P<0.05$, ** $P<0.01$, ### $P<0.01$ and *** $P<0.0001$ by one-way ANOVA analysis. Data are mean \pm s.d. BA, branchial arch.

Immunofluorescent staining confirmed these findings of p53 stabilization in the nucleus and cytoplasm when zinc is deficient (Fig. 3C).

The NE-4C cell line is derived from p53 knockout E9 neuroepithelial cells (Livingstone et al., 1992; Schlett and

Madarasz, 1997). To determine whether p53 is essential for zinc deficiency-induced apoptosis, we treated NE-4C cells with 10 μM TPEN for 1-3 h and found no difference in the number of cleaved Casp3-positive cells relative to control media (Fig. 3D,E). We then reintroduced p53 in NE-4C cells (see Materials and methods) and

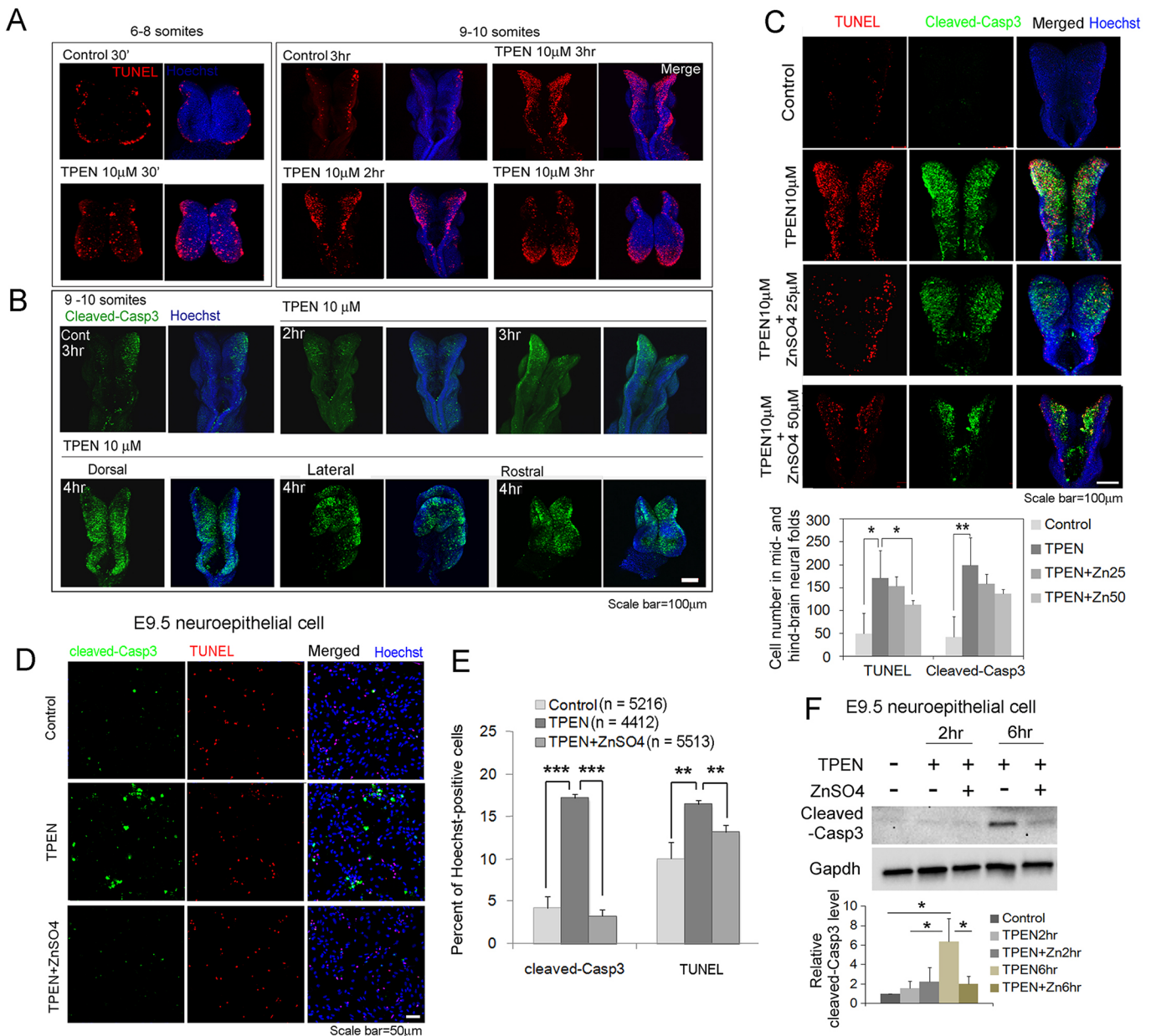


Fig. 2. Zinc deficiency increases apoptosis during neural tube closure and in neuroepithelial cells. (A-C) Typical pictures from embryos grown in roller culture show that 10 μ M TPEN treatment increases apoptosis in embryos at different developmental stages at the onset of culture (A) and apoptosis increases over time (A,B) as shown by TUNEL (red) and cleaved-Casp3 (green) staining, whereas zinc supplementation can reduce TPEN-induced TUNEL-labeled apoptosis (C, embryos were at 9 somites at start of culture). Scale bars: 100 μ m. The graph is quantitative analysis; control ($n=5$ from three independent experiments); TPEN10 μ M ($n=6$ from four independent experiments); TPEN10 μ M+ZnSO4 25 μ M ($n=3$ from two independent experiments); TPEN10 μ M +ZnSO4 50 μ M ($n=6$ from four independent experiments). * $P<0.05$ and ** $P<0.01$ by one-way ANOVA analysis. (D) TPEN increases apoptosis of E9.5 neuroepithelial cells, as shown by cleaved Casp3-positive and TUNEL-positive labeling, and apoptosis is reduced by zinc supplementation *in vitro*. Scale bar: 50 μ m. (E) Quantitative analysis of experiments as in D. ** $P<0.01$ and *** $P<0.0001$ by one-way ANOVA analysis. The data are from three independent experiments. (F) Western blot assay shows increased cleaved-Casp3 levels in E9.5 neuroepithelial cells 6 h after TPEN treatment; this is greatly reduced by zinc supplementation. Graphs show quantification of western blots. Data are mean \pm s.d. * $P<0.05$ by one-way ANOVA. All treatments were normalized to control. Data in F arise from three independent experiments.

found that 1 μ g of p53 plasmid increased the number of cleaved Casp3-positive cells, whereas 0.5 μ g did not (Fig. 3D,E). Using the lower dose of p53 (0.5 μ g), 10 μ M TPEN treatment induced an increase in cleaved Casp3 positive cells over a 3 h treatment (Fig. 3D,E). Western blot for exogenous p53 again showed stabilization of p53 levels by TPEN treatment, which was decreased to baseline levels by addition of zinc (Fig. 3F). By contrast, TPEN treatment did not impact pH3 protein levels in

NE-4C cells or brain tissue from E9.5 embryos, even when p53 levels were dramatically increased (Fig. S4B,C). These results indicate that zinc deficiency can elicit excess apoptosis through p53 stabilization.

Zinc deficiency attenuates p53 ubiquitylation

p53 stability is determined in part by its ubiquitylation (Fig. 4A). The E3 ubiquitin ligase Mdm2 ubiquitylates p53, which drives it to

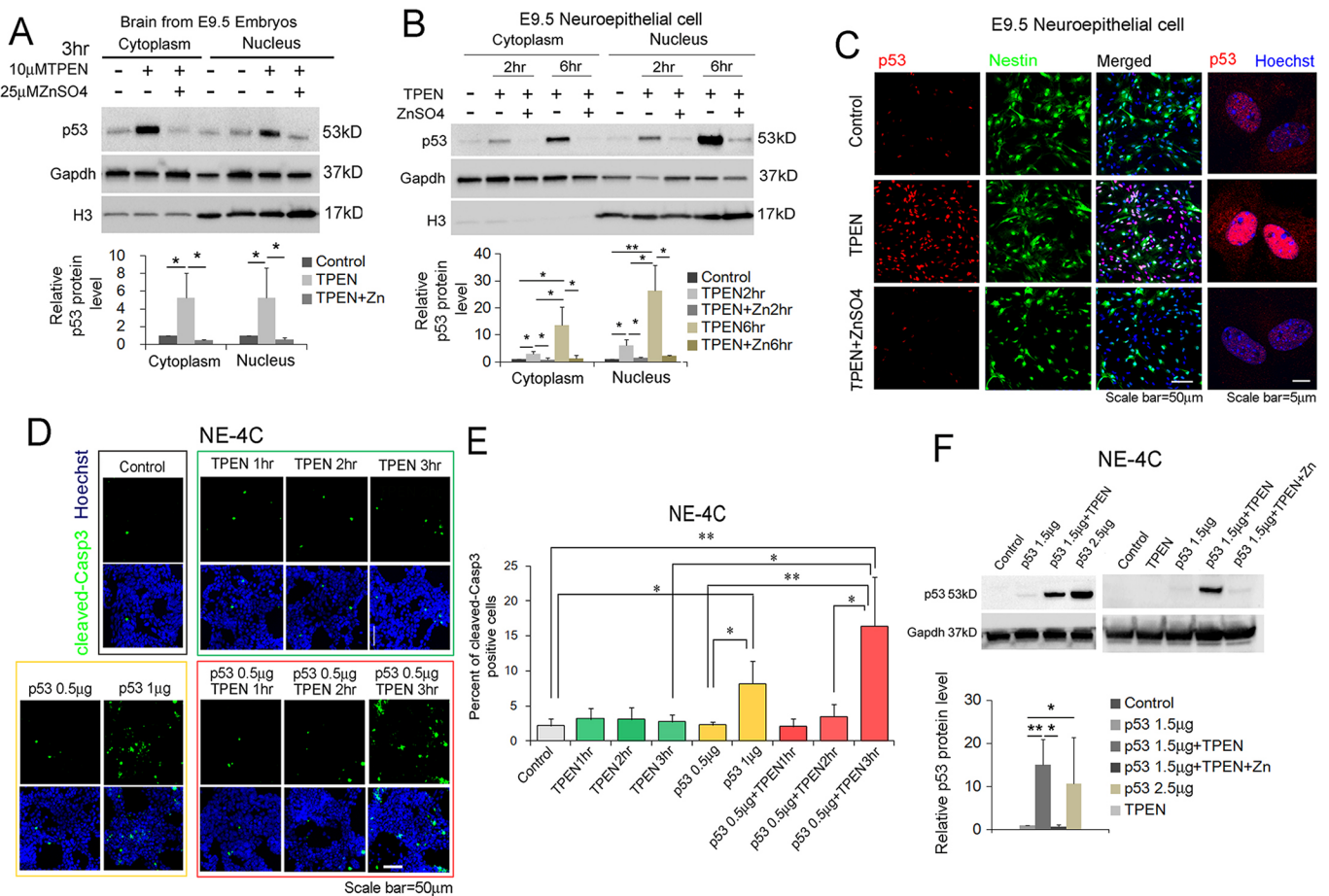


Fig. 3. p53 plays a crucial role in zinc deficiency-induced apoptosis. Western blot analysis of brain tissue from E9.5 embryos (each sample was pooled from four or five embryos, three independent experiments were performed) (A) and E9.5 primary neuroepithelial cells (from three independent experiments) (B) demonstrate that p53 levels increased in both the cytoplasm and nucleus after TPEN treatment for the indicated length of time, and p53 levels in both cellular compartments were reduced by concurrent zinc supplementation. Graphs show the corresponding quantification results of western blots. Data are mean \pm s.d. * P <0.05 and ** P <0.01 by one-way ANOVA. All treatments were normalized to corresponding control. (C) Immunofluorescence staining shows that TPEN increased p53 levels in nuclei (panels on left) and cytoplasm (panels on right; cells were grown for 6 h). (D,E) NE-4C cells, a p53-deficient E9 neuroepithelial cell line, do not respond to 10 μ M TPEN treatment (green frame in D, green bars in E), p53 re-introduction through transient transfection can induce apoptosis when given at a higher dose (1 μ g) but not a lower dose of p53 (0.5 μ g; yellow frame and yellow bars). Low-dose p53 in conjunction with TPEN can re-establish the apoptotic response of NE-4C cells and apoptosis increases over a 3 h period (red frame and red bars). One-way ANOVA analysis revealed significant differences between the groups; * P <0.05, ** P <0.01. Post-hoc Turkey HSD multiple comparison was performed (P =1.61e-05). The data were quantified from three independent experiments. (F) Western blot analysis of p53 transiently transfected NE-4C cells indicates that p53 levels were stabilized by TPEN treatment (p53 1.5 μ g versus p53 1.5 μ g+TPEN and relative to p53 2.5 μ g transfection) and p53 levels are substantially reduced by zinc supplementation (p53 1.5 μ g+TPEN+Zn). Graph shows quantification of western blots. Data are mean \pm s.d. All treatments were normalized to corresponding p53 1.5 μ g treatment. * P <0.05 and ** P <0.01 by one-way ANOVA. All data come from three to six independent experiments.

the proteasome for degradation; conversely, the deubiquitylation enzyme Hausp removes ubiquitin and stabilizes p53 (Cheng et al., 2011; Haupt et al., 1997; Li et al., 2003; Li et al., 2002; Ma et al., 2010). We first examined the level of p53 ubiquitylation in primary E9.5 neuroepithelial cells treated with a protease inhibitor MG132 and 10 μ M TPEN or TPEN+ZnSO₄, followed by p53 co-immunoprecipitation and probing with an anti-ubiquitin antibody. This revealed that the level of p53-associated ubiquitin signal was decreased after TPEN treatment, but addition of zinc recovered the levels of ubiquitylated p53 (Fig. 4B). As these experiments were performed in the presence of a proteasome inhibitor MG132, it suggests that p53 is not properly ubiquitylated upon zinc deficiency.

The N terminus of Mdm2 binds to p53 via the TAZ domain (Kussie et al., 1996), whereas its C terminus has a RING domain that requires zinc for proper assembly of Mdm2 and for its E3 ubiquitin ligase activity (Fig. 4A) (Fang et al., 2000; Nomura et al., 2017).

Moreover, in some cells, Mdm2 can be cleaved by Casp3 at amino acid residue 359 or 361 to produce a short isoform of Mdm2 (~60 kDa) that lacks the C-terminal RING domain (Erhardt et al., 1997; Pochampally et al., 1998). To determine whether zinc deficiency affects the interaction between p53 and Mdm2, we performed p53 co-immunoprecipitation assays on brain tissue from E9.5 embryos treated for 3 h with 10 μ M TPEN or TPEN+Zn. This showed that binding of p53 to the full-length isoforms of Mdm2 (~130 and ~90 kDa) was significantly reduced by TPEN treatment, and this interaction could be restored by zinc supplementation (Fig. 4C,D). In contrast, binding of p53 to the short isoform of Mdm2 (~55 kDa) was not affected by zinc deficiency, and the levels of total protein of the short isoform was dramatically increased (Fig. 4C,D). Similarly, in primary E9.5 neuroepithelial cells, 2 h after TPEN treatment, the binding of p53 to Mdm2 (~90 kDa) was strongly diminished but p53 binding to the short isoform (~55 kDa) was

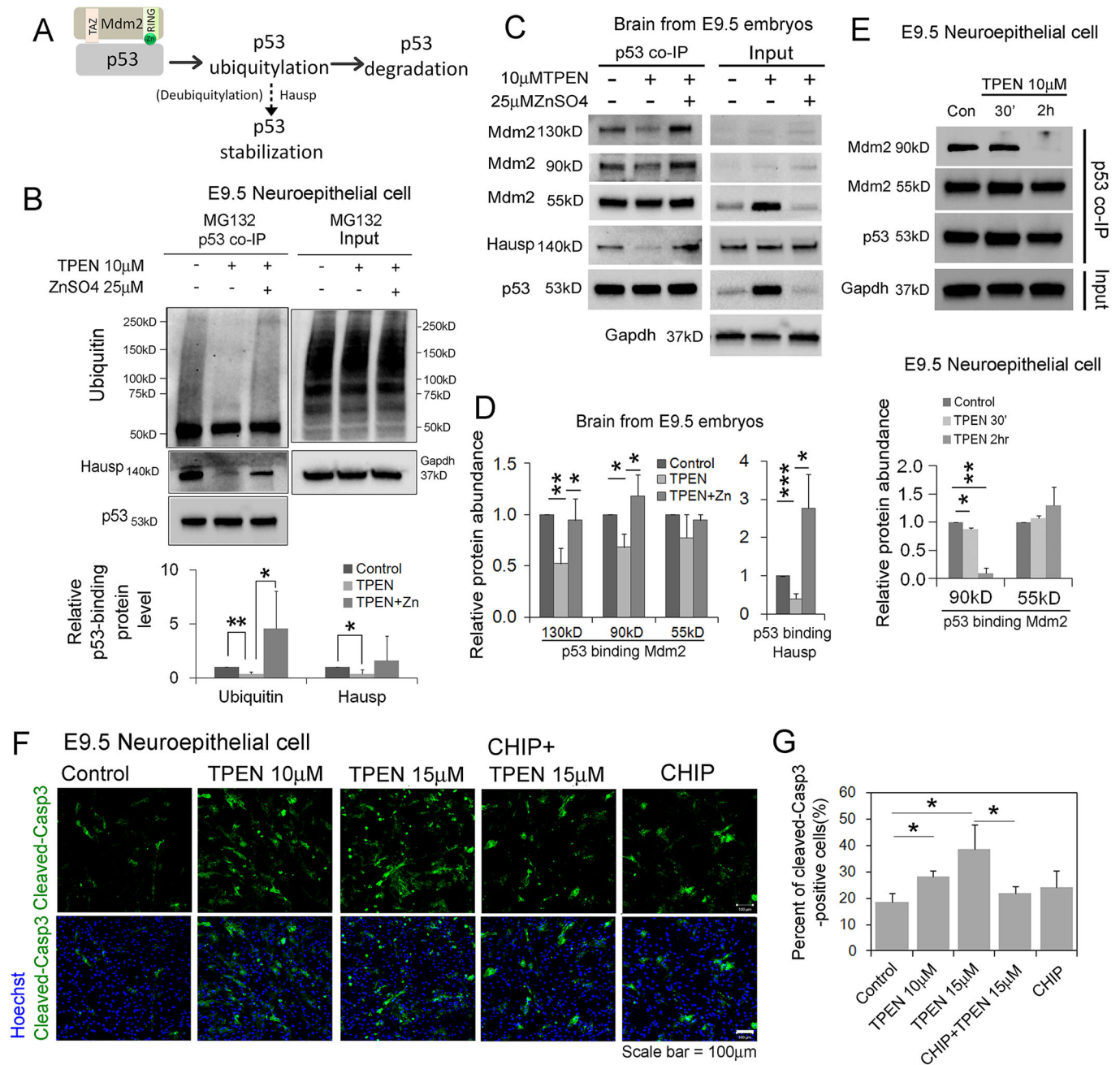


Fig. 4. Zinc deficiency attenuates p53 ubiquitylation. (A) Schematic of the regulation of p53 ubiquitylation by the zinc-regulated E3 ubiquitin ligase Mdm2 and by the p53-deubiquitylating enzyme Hausp, leading to p53 degradation or stabilization. The N terminus of Mdm2 binds p53 via a TAZ domain, whereas the C-terminal zinc-regulated RING domain is required for ubiquitin ligase activity towards p53. TAZ, transactive zone. (B) E9.5 primary neuroepithelial cells treated with MG132 proteasome inhibitor and TPEN or TPEN+ZnSO₄, followed by p53 co-immunoprecipitation and western blot analysis with antibodies against ubiquitin and Hausp shows TPEN decreases p53 ubiquitylation and Hausp binding. Graph shows western blot quantification data. Immunoprecipitated p53 is used as a loading control. Data are mean±s.d. All treatments were normalized to control. **P*<0.05, ***P*<0.01 by one-way ANOVA analysis. All data came from three independent experiments. (C,D) Typical western blot images (C) and quantification (D) of the different forms of Mdm2 and of Hausp following p53 co-immunoprecipitation of brain tissue from E9.5 embryos treated for 3 h in control media or in media containing 10 μM TPEN or 10 μM TPEN+25 μM ZnSO₄. In the early embryonic brain we detected full-length Mdm2 (~130 kDa and ~90 kDa) and cleaved Mdm2 in which the C terminus is removed (~55 kDa). All Mdm2 protein forms are bound by p53 in the presence or absence of zinc, but p53 shows reduced binding to full-length Mdm2 isoforms. Hausp binding to p53 is much decreased upon TPEN treatment, despite p53 stabilization (input lane). Immunoprecipitated p53 is used as a loading control. Data are mean±s.d. All treatments were normalized to control. **P*<0.05, ***P*<0.01 and ****P*<0.0001 by one-way ANOVA analysis. Each sample was pooled from four or five embryos, all data arise from three independent experiments. (E) Typical gel images of E9.5 primary neuroepithelial cells cultured for 30 min or 2 h in control media or TPEN, followed by p53 co-immunoprecipitation and western blot analysis for Mdm2. Western blot results were quantified (graph). Immunoprecipitated p53 is used as a loading control. Data are mean±s.d. All treatments were normalized to control. **P*<0.05 and ***P*<0.01 by one-way ANOVA analysis. All data arise from two independent experiments. (F,G) CHIP, a zinc-independent E3 ubiquitin ligase of p53, was overexpressed in E9.5 neuroepithelial cells, followed by TPEN treatment for 6 h. CHIP overexpression reduced the number of cleaved Casp3-positive cells, as determined by immunofluorescent staining (F) and quantified in G. **P*<0.05 by one-way ANOVA analysis. Data are mean±s.d. All data arise from three independent experiments.

unchanged (Fig. 4E). The deubiquitylation enzyme Hausp also binds to ubiquitylated p53 and this binding was attenuated by TPEN treatment, whereas the addition of zinc increased p53 ubiquitylation and binding between p53 and Hausp (Fig. 4B-D). Taken together, these data suggest that zinc deficiency stabilizes p53 by disrupting Mdm2-mediated p53 ubiquitylation rather than increasing the interaction with Hausp deubiquitylation enzyme.

As a further test that the zinc deficiency-induced attenuation of p53 ubiquitylation allows a stabilization of p53 activity and leads to initiation of apoptosis, we manipulated the system with human CHIP (STUB1), a zinc-independent E3 ubiquitin ligase of p53 (Esser et al., 2005). CHIP overexpression in primary E9.5 neuroepithelial cells or in p53-transfected NE-4C cells can attenuate TPEN-induced p53 stabilization (Fig. S5A,B). Importantly, when CHIP was overexpressed in primary neuroepithelial cells, the TPEN-induced increase in cleaved Casp3-positive cells was significantly reversed (Fig. 4F,G). Taken together, we interpret these findings as indicating that zinc deficiency-induced p53 stabilization is due to reduced p53 ubiquitylation as a consequence of disruption of the zinc-coordinating RING domain of Mdm2, which leads to excess apoptosis during the process of neural tube closure.

Zinc deficiency enhances p53 transcription activity

p53 plays dual functions in the promotion of apoptosis: one as a transcription factor to regulate apoptosis-relevant target genes; the other by directly binding to anti-apoptotic Bcl2/Bcl-xl proteins to release pro-apoptotic mitochondrial Bax (Marchenko and Moll, 2007; Mihara et al., 2003; Toledo and Wahl, 2006; Vaseva and Moll, 2009). To attempt to discover the pathway affected by zinc deficiency-induced p53 stabilization during neural tube closure, we used two well-established pharmacological inhibitors of p53: pifithrin- α , an inhibitor of p53 transcriptional activity (Komarov et al., 1999; Sohn et al., 2009); and pifithrin- μ , which inhibits the p53 mitochondrial pathway and HSP70 (Sekihara et al., 2013; Strom et al., 2006). Time-lapse live imaging of 9-somite *Ven^{myr}* mouse embryos revealed that 40 μ M pifithrin- α can clearly rescue TPEN-induced failure of neural tube closure (closure by 11 h \pm 27 min; $n=6$; Fig. 5A,B, Movie 4). In contrast, pifithrin- μ (50 μ M) failed to promote neural tube closure ($n=5$; Fig. 5A,B, Movie 5). These results suggest that p53 transcriptional activity is the main pathway deployed in the context of zinc deficiency, leading to NTD. The features of neural fold inflection were significantly improved by pifithrin- α co-treatment with TPEN and became similar to control (Fig. 5C-F). Moreover, pifithrin- α reduced the TPEN-induced increase in cleaved Casp3-positive cells in the midbrain and hindbrain regions in 9- to 10-somite embryos (Fig. 5G). Analysis of gene expression changes in primary E9.5 neuroepithelial cells showed that TPEN increased the expression of p53 target genes: the pro-apoptotic genes *Fas1* (*Fas*) and *Bax*, as well as *Mdm2* which is transcriptionally regulated by p53 in a negative feedback loop (Fig. 5H-J), but not the *Cdkn1a* gene, which encodes a cell cycle arrest protein p21^{Cip1} that is targeted by p53 (Fig. 5K) (el-Deiry et al., 1993). These p53 target pro-apoptotic genes were returned to normal levels by TPEN+ZnSO₄ treatment (Fig. 5H-J). These data indicate that p53 transcriptional activity predominates in the promotion of apoptosis when zinc is deficient, resulting in failure of neural tube closure.

DISCUSSION

Zinc is an essential nutritional trace element during neural development

Epidemiological data in humans has implicated zinc deficiency as a risk factor for NTDs. Here, we sought to develop a mouse model of

zinc deficiency to explore the cellular and molecular basis for failure of neural tube closure. A distinct advantage of our system, in which zinc levels are manipulated acutely, is that we can evaluate the immediate direct response, versus potential indirect consequences. We demonstrate that acute zinc deficiency in embryos causes excessive cell death, starting within 1 h and increasing thereafter, and ultimately results in failure of neural tube closure. Moreover, using live imaging, we find that neural fold zipping is not grossly affected but inflection of the neural folds towards each other is disrupted, preventing the neural folds from meeting at the midline. The early embryonic neuroepithelium appears most sensitive to zinc deficiency. Consistent with our findings of neural cell death, others have shown that reduced zinc conditions lead to cell death of neuroepithelial cells in embryos from wild-type dams given a zinc-deficient diet (Dufner-Beattie et al., 2006; Harding et al., 1988), in neuroblastoma and neural progenitor-like cells (Adamo et al., 2010; Nuttall et al., 2015; Seth et al., 2015), in adult neural stem cells (Corniola et al., 2008), and in cortical neurons (Adamo et al., 2010; Ra et al., 2009). Other effects of zinc deficiency include: reduced expression of the neural stem cell marker nestin in embryos and pups from dams fed a severely zinc-deficient diet (Wang et al., 2001); altered neural differentiation of neural precursor cells induced to differentiate with retinoic acid (Morris and Levenson, 2013) and of human induced pluripotent stem cells differentiated to motor neurons (Pfaender et al., 2016); and decreased fetal (rat E19) neural progenitor cell proliferation (Nuttall et al., 2015). Adult mice fed a zinc-deficient diet for 5 weeks show a decrease in proliferating neural cells and immature neurons, and apoptosis in the hippocampus (Gao et al., 2009). However, our acute embryonic zinc-deficiency studies did not detect a change in cell proliferation, although it is possible that longer periods of zinc deficiency may disrupt proliferation of these early neural progenitor cells. Zinc dyshomeostasis, either an excess or deficiency, is also implicated as a risk factor for neurodegenerative disorders (Szewczyk, 2013). Together, the data highlight zinc homeostasis as being crucial for neural development from embryonic through adult neurogenesis. Our *in vivo* and *in vitro* results of the earliest neural progenitor cells implicate apoptosis as the predominant phenotype associated with zinc deficiency-induced NTDs.

Zinc deficiency disrupts neural tube closure through p53 stabilization

Our results that include rescue experiments point to p53 as being an important mediator of the apoptotic phenotype, although we are aware that the full response to zinc deficiency is likely molecularly complex and broader than the studies here have covered. Indeed, others have suggested that zinc deficiency alters binding activity of transcription factors involved in neuronal differentiation (Gower-Winter et al., 2013; Morris and Levenson, 2013), and decreases proliferation by reducing ERK1/2 signaling (Nuttall et al., 2015).

Here, we provide another mechanism related to p53 stabilization, through disruption of Mdm2 activity, for consideration of zinc function in neuroepithelial progenitor cells. Earlier studies found that p53 is stabilized when zinc is deficient (Ra et al., 2009). Our studies support this finding and extend it to an *in vivo* context and add mechanistic insight. In the developing mouse embryo, we found that acute zinc deficiency stabilizes p53 through disruption of its ubiquitylation. This increases p53 levels and causes excessive apoptosis and NTD, consistent with the role of p53 in regulating the response to cellular stress and initiating apoptosis.

p53 protein levels in embryonic neural tissue and primary neuroepithelial cells increase within 2 h of TPEN-induced zinc

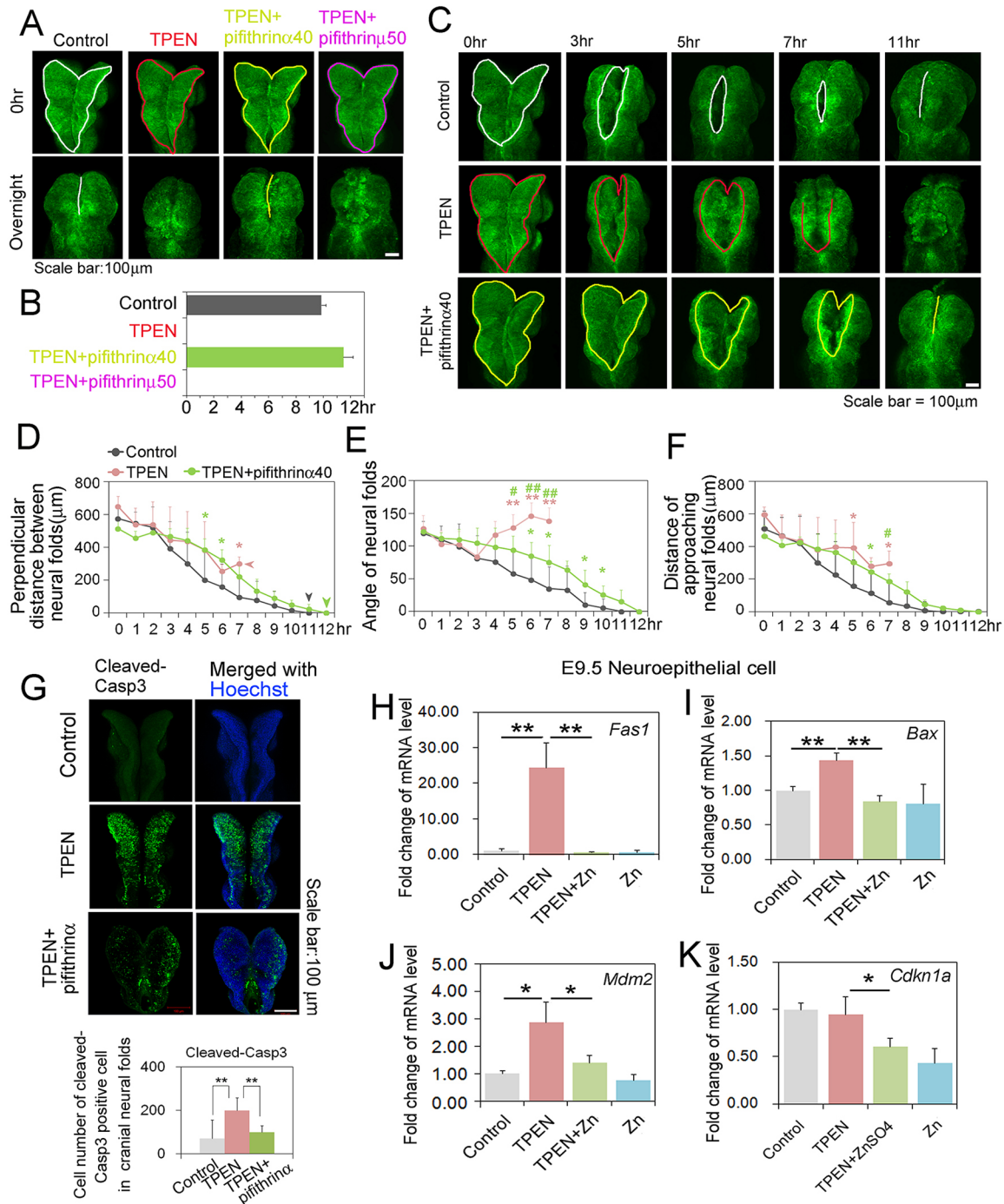


Fig. 5. Inhibition of p53 transactivation function overcomes zinc deficiency-induced failure of neural tube closure. (A) Still frames from time-lapse live imaging of E8.5 *Ven^{Myr}* embryos show that an inhibitor of p53 transactivation function, pifithrin- α , but not an inhibitor of p53 mitochondrial function, pifithrin- μ , can rescue TPEN-induced failure of neural tube closure. (B) Time to neural tube closure after TPEN+pifithrin- α ($n=6$ from three independent experiments) relative to control ($n=6$ from four independent experiments) (the neural tube never closes with TPEN treatment) ($n=6$ from two independent experiments) or TPEN +pifithrin- μ -treated embryos ($n=5$ from two independent experiments). (C-F) Representative still images (C) and quantitative data (D-F) of time-lapse imaging show the ability of pifithrin- α to rescue TPEN-induced failure of neural tube closure. In A and C, the white lines, red lines, yellow lines and purple line show the edges of neural folds. In D, the pink arrowhead indicates failure of neural tube closure; the dark gray and green arrowheads indicate the timepoint of neural tube closure. * $P<0.05$ (TPEN versus control), * $P<0.05$ (TPEN+pifithrin α 40 versus control), # $P<0.05$ (TPEN+pifithrin α 40 versus TPEN). * $P<0.05$, # $P<0.05$, ** $P<0.01$ and ## $P<0.01$ by one-way ANOVA analysis. (G) E8.5 embryos grown in roller culture for 3 h indicate that pifithrin- α inhibits TPEN-induced apoptosis, as shown by the reduced number of cleaved Casp3-positive cells, quantified in the graph. ** $P<0.01$ by one-way ANOVA analysis. Control ($n=5$ from five independent experiments), TPEN ($n=6$ from four independent experiments) and TPEN+pifithrin α ($n=9$ from three independent experiments). (H-K) Real-time qPCR assays of E9.5 primary neuroepithelial cells show that TPEN induces the expression of p53 transcription targets, including the apoptotic genes *Fas1*, *Bax* and *Mdm2*, but not the cell cycle arrest gene *Cdkn1a*. Zinc supplementation can rescue the TPEN-induced increases in p53 apoptosis target genes; * $P<0.05$ and ** $P<0.01$ by one-way ANOVA analysis. Data are mean \pm s.d. All data arise from three biological replicates. pifithrin α 40, 40 μ M pifithrin- α ; pifithrin μ 50, 50 μ M pifithrin- μ .

deficiency. This relatively rapid response suggests that p53 accumulation is due to inhibition of p53 degradation. p53 degradation is mediated by ubiquitylation of p53, which targets it to the proteasome. We find that p53 ubiquitylation is greatly reduced upon zinc deficiency. Mdm2 is the major E3 ubiquitin ligase for p53 and Mdm2 ubiquitylation activity is zinc dependent (Fang et al., 2000; Nomura et al., 2017; Shloush et al., 2011). Our results, in combination with biochemical studies of others, suggest that Mdm2 E3 ligase function is disrupted as a result of attenuated Mdm2 assembly and Mdm2 RING domain activity upon zinc deficiency. We show that zinc deficiency reduced binding of full-length Mdm2 to p53, and resulted in cleavage of Mdm2 to a shorter isoform without E3 ligase activity. It is likely that the culmination of these zinc-deficiency mediated changes to Mdm2 is responsible for the reduction in p53 ubiquitylation that results in p53 stabilization.

Zinc deficiency results in increased p53 in the cytoplasm and in the nucleus. We postulate that the increase in the nucleus is from two sources. First, translocation of stabilized p53 from the cytoplasm to the nucleus, consistent with results in which zinc-deficient conditions cause p53 translocation from the cytoplasm to the nucleus (Corniola et al., 2008). Second, inhibition of p53 nuclear export, as this is mediated by the Mdm2 zinc-coordinating RING-finger domain (Geyer et al., 2000). Zinc deficiency decreases the levels of the full-length RING-finger domain containing isoform of Mdm2 and attenuates binding of p53 to this isoform. Therefore, zinc deficiency would be predicted to decrease p53 nuclear export, and indeed we find an increase of p53 in the nucleus upon TPEN treatment of E9.5 neuroepithelial cells both *in vivo* and *in vitro* (Fig. 3A-C).

Excess p53 transcription activity underlies zinc deficiency-induced neural tube defects

Consistent with an increase of p53 in the nucleus upon TPEN treatment, we also observed increased expression of p53 target genes (Fig. 5H-J). To distinguish between zinc deficiency-induced p53-mediated apoptosis due to p53 transcriptional activity or mitochondrial pro-apoptotic function, we used pharmacological

inhibitors specific to each of these pathways. Although we cannot rule out a possible role for the mitochondrial pathway, our results clearly show that inhibition of p53 transcription activity is sufficient to prevent the TPEN-induced NTD. We also observe a robust increase of p53 in the nucleus upon TPEN treatment (Fig. 3A-C), where it can then act as a transcription factor. Our studies show zinc deficiency induces the expression of p53 pro-apoptotic target genes *Bax* and *Fas1*, as well as *Mdm2*, which is autoregulated by p53, consistent with previous studies (Gao et al., 2009; Seth et al., 2015). Furthermore, the ability of the p53 transcriptional inhibitor to relieve zinc deficiency-induced apoptosis and to restore neural tube closure provides evidence that increased p53 transcriptional activity, due to disruption of Mdm2-regulated p53 stabilization and nuclear accumulation, is responsible for the zinc deficiency-induced NTDs.

Zinc is indispensable for multiple molecular events relevant to p53. The DNA-binding domain (DBD) of p53 contains zinc and the level of zinc ions is crucial for proper DBD folding and p53 DNA-binding activity (Butler and Loh, 2003, 2007; Duan and Nilsson, 2006). This might predict that zinc deficiency would decrease p53 DNA-binding activity and lead to a decrease in apoptosis. However, our *in vivo* data over a relatively short timescale of zinc deficiency indicate that p53 target gene expression is enhanced and apoptosis is increased, suggesting that at least the acute effect of zinc deficiency in the neuroepithelium is not mediated via an effect on the p53 DBD.

Our model of at least one predominant effect of zinc on neural tube closure is schematized in Fig. 6. During normal neural tube closure, when zinc levels are adequate, the p53-Mdm2 relationship is intact, allowing Mdm2 to modulate p53 levels to maintain cell survival and inhibit cell death. Our study highlights a mechanistic pathway in which zinc deficiency leads to failure of neural tube closure through attenuation of p53 ubiquitylation by Mdm2, p53 stabilization, increased p53 nuclear accumulation, enhancement of p53 transcriptional activity and initiation of extensive cell death, which prevent the neuroepithelial folds from continuing their progress towards the dorsal midline to meet and form a closed neural tube.

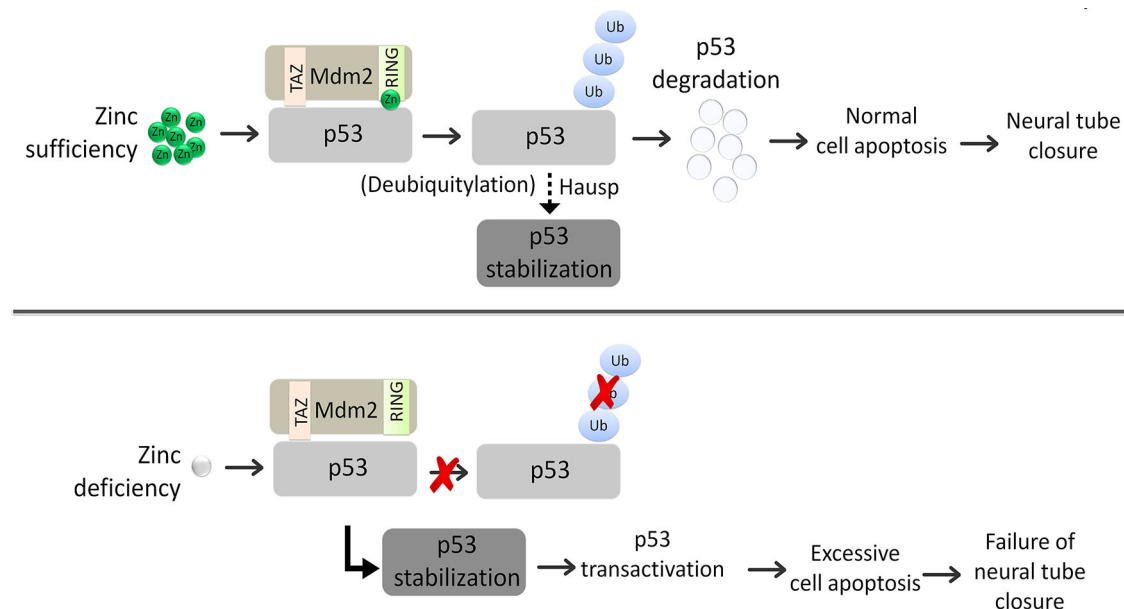


Fig. 6. Model for the proposed mechanism of zinc deficiency-induced failure of neural tube closure. In the presence of zinc, Mdm2 protein can bind and ubiquitylate p53, resulting in p53 degradation, maintenance of cell survival and proper neural tube closure. Zinc deficiency attenuates Mdm2 binding and activity toward p53, resulting in p53 stabilization and an increase in p53 transcriptional activity, causing cell death and failure of neural tube closure.

MATERIALS AND METHODS

Mice and whole-embryo culture and imaging system

C57BL/6J mice were used for E9.5 brain tissue collection and primary E9.5 neuroepithelial cell isolation. Transgenic mice CAG::myr-venus (Rhee et al., 2006) [Jackson Labs Tg(CAG-Venus)^{1Hadj/J}] were used for time-lapse live imaging data collection. All mice were housed at the University of Colorado Anschutz Medical Campus in accordance with an IACUC approved protocol.

As described in our previous publications (Massarwa and Niswander, 2013; Ray and Niswander, 2016), somite-staged embryos were placed in culture media on a mounting platform for imaging on a Zeiss LSM 880 Meta confocal microscope on a motorized stage with a temperature- and gas-controlled incubator (37°C, 5% O₂, 5% CO₂). Culture medium was DMEM without Phenol Red and contained 55 U/ml penicillin/streptomycin, 2.2 mM glutamax, 11 mM Hepes buffer, mixed with 75% rat serum (Harlan, #B-4520). The embryos were mounted on black Millipore filter paper (AABG01300). Glass-bottomed dishes were from MatTek (P35G-1.5-20-C). Images were acquired using a 10× lens c-Apochromat NA1.2 with 0.7 digital zoom out. A 448 nm laser (around 2% power) was used. Images were acquired at 512×512 resolution. The thickness of z-slices was 15 μm (a total of 15–30 slices/time point, depending on the experiment). The time interval for imaging was ~5 min. Post-imaging processing and measurements were carried out using the LSM image browser (Zeiss 880). The movies were exported using Imaris 8.0 software.

For molecular studies, E8.5 or E9.5 embryos were dissected with intact yolk sac and placed in a roller culture system similar to that used by Pyrgaki et al. (2010) in a gas-controlled incubator (37°C, 5% O₂, 5% CO₂). The same culture medium as above was mixed with 50% rat serum. Embryos were treated for 30 min to 4 h in Fig. 2A,B, for 4 h in Fig. 2C, for 3 h in Fig. 3A and for 3 h for experiments in Fig. 4C,D. For western blot and co-IP assays, brain tissues from four or five embryos exposed to the same treatment were pooled for protein extraction as one sample.

Cell culture

E9.5 neuroepithelial cells were dissected from whole-brain tissue of E9.5 mouse embryos and pipetted up and down to dissociate cells. The culture medium was as previously published for E8.5 neuroepithelial cells (Tropépe et al., 1999) using a chemically defined serum-free basic medium composed of a 1:1 mixture of Dulbecco's modified Eagle's medium (DMEM; 11995, GIBCO) and F-12 nutrient (11765-054, GIBCO) including 0.6% glucose (D9434, Sigma), 2 mM glutamine (25030081, GIBCO), 3 mM sodium bicarbonate (25080, GIBCO), 5 mM HEPES buffer (15630, GIBCO), 25 μg/ml insulin (I9278, Sigma), 100 μg/ml transferrin (T8158, Sigma), 20 nM progesterone (P6149, Sigma), 60 μM putrescine (P5780, Sigma) and 30 nM selenium chloride (323527, Sigma). FGF2 (10 ng/ml) (SRP4037, Sigma), 2 μg/ml heparin (H3149, Sigma) and 20 ng/ml EGF (62253-63-8, Sigma) were added into the basic medium as a growth medium. NE-4C cells (ATCC #CRL-2925) were grown at 37°C and 5% CO₂ in MEM (Invitrogen) supplemented with 5% FBS, 1×MEM nonessential amino acids (Invitrogen) and 1×GlutaMax (Invitrogen). The NE-4C cell line has been tested in the lab for mycoplasma contamination.

Drug treatment

To establish a zinc-deficient environment, N,N,N',N'-Tetrakis (2-pyridylmethyl) ethylenediamine (TPEN) (P4413, Sigma) was dissolved in DMSO and used at a final concentration of 10 μM or 15 μM to treat cells or embryos according to the previous studies in which 1–100 μM were employed (Gao et al., 2017; Rayman et al., 2018; Strand et al., 2013). For zinc supplementation, zinc sulfate heptahydrate (Z4750, Sigma) was dissolved in water and used at a final concentration of 25 μM or 50 μM ZnSO₄ (Gao et al., 2017). Pifithrin-α (1267, Tocris) and pifithrin-μ (2653, Tocris) were used to inhibit p53 transcriptional activity and the mitochondrial pro-apoptotic pathway, respectively. Pifithrin-α and pifithrin-μ were dissolved in DMSO and used at a final concentration of 40 μM for pifithrin-α and 50 μM for pifithrin-μ according to previous studies in which 3–100 μM pifithrin-α (Komarov et al., 1999; Sohn et al., 2009) and 10–50 μM pifithrin-μ were employed (Strom et al., 2006).

Western blot

The cytoplasm and nuclei were fractionated using a Nuclear Complex Co-IP kit (54001, Active Motif). Proteins extracts were subjected to polyacrylamide gel electrophoresis and electrotransfer to PVDF membranes. The membranes were blocked with 5% non-fat milk and then probed with the indicated antibodies in TBS-Tween 20. Antibodies used were against p53 (1C12) (1:500; 2524; Cell Signaling Technology); cleaved caspase 3 (Asp175) (1:500; 9661; Cell Signaling Technology); Hausp (D17C6) (1:500; 4833; Cell Signaling Technology); Mdm2 (SMP14) (1:50; sc-965; Santa Cruz); Chip (C3B6) (1:500; 2080; Cell Signaling Technology); ubiquitin (1:500; 3933; Cell Signaling Technology); DDK (FLAG OTI4C5) (1:2000; TA50011; Origene); pH3 (1:500; 9714; Cell Signaling Technology) H3 (1:14,000; ab1791; Abcam); and Gapdh (Sigma; G9545; 1:2000). ImageJ was used to quantify the western blot data. Integrated gray value was measured. In all assays, relative protein level was standardized by dividing the referenced protein (usually Gapdh in cytoplasm or H3 in the nucleus), and then one treatment was designated as 1, and the other treatments were normalized to this treatment.

Co-immunoprecipitation

Freshly dissected embryonic brain tissue or E9.5 neuroepithelial cells were collected, and total protein was harvested. Anti-p53 (1C12) antibody (2524; Cell Signaling Technology) (5 μl) was added to 500 μg of input and rotated overnight at 4°C. Washed PureProteome Protein A/G Mix Magnetic Beads (50 μl; LSKMAGAG02; Millipore) were added and samples incubated at 4°C for 1 h on a rotator. Beads were washed five times in ice-cold wash buffer before elution in 2× Laemmli buffer at 95°C for 10 min. Protein interactions were subsequently assayed via western blot and ImageJ was used to quantify the data. In all assays, relative protein level was standardized by dividing the p53 protein level in immunoprecipitated protein, and then one treatment was designated as 1, the other treatments were normalized to this treatment.

Plasmid transfection

To reintroduce p53 or overexpress CHIP protein, NE-4C cells or E9.5 primary neuroepithelial cells were subjected to transient transfection. Plasmids containing the coding region of human p53 (*TP53*-Myc-DDK-tagged) (RC200003, Origene) or human CHIP protein (*STUB1*-Myc-DDK-tagged) (RC200310, Origene) were transfected into cells using Xfect Transfection Reagent (Clontech) according to the manufacturer's protocol (1.5 μg or 2.5 μg plasmid for transfection per well of a 12-well plate; 0.5 or 1 μg for 24-well plate). Approximately 24 h after transfection, 15 μM TPEN was added and the cultures collected 1–3 h later for immunofluorescent staining or western blot analysis.

Immunofluorescent staining, TUNEL assays and confocal microscopy

Embryos or cultured cells were fixed for 10–15 min at room temperature in 4% PFA, blocked for 1 h at room temperature, and stained with primary antibody overnight at 4°C. Primary antibodies used were as follows: p53 (1C12) (1:300; 2524; Cell Signaling Technology); cleaved caspase 3 (Asp175) (1:300; 9661; Cell Signaling Technology); nestin (SP103) (1:100; ab105389; Abcam); pH3 (1:300; 9714; Cell Signaling Technology). Hoechst (1:1000)-labeled nuclei were counted as a cell number control.

In Situ Cell Death Detection Kit (12156792910; Roche) was used for TUNEL assays. Embryos or cultured cells were fixed by 4% paraformaldehyde for 10–15 min at room temperature, then a TUNEL-labeled assay was performed following the manufacturer's instructions.

Imaging was performed on a Zeiss LSM880 Meta laser scanning confocal microscope using Zen software. Imaris 8.0 software was used for cell counting quantitative analysis. The number of Hoechst-labeled cells in a field were counted and the percentage of cleaved-Casp3 or TUNEL-positive cells quantified. In embryos, the number of cleaved Casp3-positive, TUNEL-positive or pH3-positive cells were counted in hindbrain and midbrain regions.

Real-time qRT-PCR

E9.5 primary neuroepithelial cells were harvested 6 h after 15 μM TPEN or 15 μM TPEN+ 25 μM ZnSO₄, or 25 μM ZnSO₄ treatment. RNA was

isolated according to manufacturer's instructions using the High Pure RNA Isolation Kit (Roche) and cDNA was generated using random hexamers and the Transcriptor First Strand cDNA Synthesis Kit (Roche). qPCR was performed on a LightCycler 480 (Roche) using the LightCycler 480 Probes Master reagent (Roche) and Universal Probe Library (Roche) according to the manufacturer's protocol. All primers and probes are listed in Table S1. Data were collected and analyzed with LightCycler 480 Software (Roche; Version 1.5.1). *Actb* gene is referenced gene. All experiments were from three biological replicates.

Statistical analysis

One-way ANOVA was used to analyze the experimental data, post-hoc Tukey HSD multiple comparisons were performed in multiple treatment assays. Values are represented as mean±s.d.; $P < 0.05$ is considered as statistically significant.

Acknowledgements

We thank our lab for constructive advice and James Orth for critical reading of the manuscript.

Competing interests

The authors declare no competing or financial interests.

Author contributions

Conceptualization: H.L., L.N.; Methodology: H.L.; Investigation: H.L., J.Z.; Writing - original draft: H.L.; Writing - review & editing: H.L., L.N.; Visualization: H.L., L.N.; Supervision: L.N.; Funding acquisition: L.N.

Funding

This work was supported by the Children's Hospital Colorado and National Institutes of Health/National Institute of Child Health and Human Development grants R01HD081562 and R01HD081117. Deposited in PMC for release after 12 months.

Supplementary information

Supplementary information available online at <http://dev.biologists.org/lookup/doi/10.1242/dev.169797.supplemental>

References

- Adamo, A. M., Zago, M. P., Mackenzie, G. G., Aimo, L., Keen, C. L., Keenan, A. and Oteiza, P. I. (2010). The role of zinc in the modulation of neuronal proliferation and apoptosis. *Neurotox. Res.* **17**, 1-14.
- Andreini, C., Banci, L., Bertini, I. and Rosato, A. (2006). Counting the zinc-proteins encoded in the human genome. *J. Proteome Res.* **5**, 196-201.
- Andrews, G. K., Wang, H., Dey, S. K. and Palmiter, R. D. (2004). Mouse zinc transporter 1 gene provides an essential function during early embryonic development. *Genesis* **40**, 74-81.
- Buamah, P. K., Russell, M., Bates, G., Ward, A. M. and Skillen, A. W. (1984). Maternal zinc status: a determination of central nervous system malformation. *Br. J. Obstet. Gynaecol.* **91**, 788-790.
- Butler, J. S. and Loh, S. N. (2003). Structure, function, and aggregation of the zinc-free form of the p53 DNA binding domain. *Biochemistry* **42**, 2396-2403.
- Butler, J. S. and Loh, S. N. (2007). Zn(2+)-dependent misfolding of the p53 DNA binding domain. *Biochemistry* **46**, 2630-2639.
- Cai, C. and Shi, O. (2014). Genetic evidence in planar cell polarity signaling pathway in human neural tube defects. *Front. Med.* **8**, 68-78.
- Cameron, I. L. and Greulich, R. C. (1963). Evidence for an essentially constant duration of DNA synthesis in renewing epithelia of the adult mouse. *J. Cell Biol.* **18**, 31-40.
- Carrillo-Ponce Mde, L., Martinez-Ordaz, V. A., Velasco-Rodriguez, V. M., Hernandez-Garcia, A., Hernandez-Serrano, M. C. and Sanmiguel, F. (2004). Serum lead, cadmium, and zinc levels in newborns with neural tube defects from a polluted zone in Mexico. *Reprod. Toxicol.* **19**, 149-154.
- Cavdar, A. O., Bahceci, M., Akar, N., Erten, J., Bahceci, G., Babacan, E., Arcasoy, A. and Yavuz, H. (1988). Zinc status in pregnancy and the occurrence of anencephaly in Turkey. *J. Trace Elem. Electrolytes. Health Dis.* **2**, 9-14.
- Çavdar, A. O., Bahceci, M., Akar, N., Dincer, F. N. and Erten, J. (1991). Maternal hair zinc concentration in neural tube defects in Turkey. *Biol. Trace Elem. Res.* **30**, 81-85.
- Cengiz, B., Söylemez, F., Öztürk, E. and Cavdar, A. O. (2004). Serum zinc, selenium, copper, and lead levels in women with second-trimester induced abortion resulting from neural tube defects: a preliminary study. *Biol. Trace Elem. Res.* **97**, 225-235.
- Cheng, Q., Cross, B., Li, B., Chen, L., Li, Z. and Chen, J. (2011). Regulation of MDM2 E3 ligase activity by phosphorylation after DNA damage. *Mol. Cell. Biol.* **31**, 4951-4963.
- Cho, Y.-E., Lomeda, R.-A., Ryu, S.-H., Lee, J.-H., Beattie, J.-H. and Kwun, I.-S. (2007). Cellular Zn depletion by metal ion chelators (TPEN, DTPA and chelex resin) and its application to osteoblastic MC3T3-E1 cells. *Nutr. Res. Pract.* **1**, 29-35.
- Copp, A. J., Stanier, P. and Greene, N. D. E. (2013). Neural tube defects: recent advances, unsolved questions, and controversies. *Lancet Neurol.* **12**, 799-810.
- Copp, A. J., Adzick, N. S., Chitty, L. S., Fletcher, J. M., Holmbeck, G. N. and Shaw, G. M. (2015). Spina bifida. *Nat. Rev. Dis. Primers* **1**, 15007.
- Corniola, R. S., Tassabehji, N. M., Hare, J., Sharma, G. and Levenson, C. W. (2008). Zinc deficiency impairs neuronal precursor cell proliferation and induces apoptosis via p53-mediated mechanisms. *Brain Res.* **1237**, 52-61.
- Czeizel, A. E. (1993). Prevention of congenital abnormalities by periconceptional multivitamin supplementation. *BMJ* **306**, 1645-1648.
- Czeizel, A. E. and Dudás, I. (1992). Prevention of the first occurrence of neural-tube defects by periconceptional vitamin supplementation. *N. Engl. J. Med.* **327**, 1832-1835.
- Czeizel, A. E., Dudas, I. and Météneki, J. (1994). Pregnancy outcomes in a randomised controlled trial of periconceptional multivitamin supplementation. Final Report. *Arch. Gynecol. Obstet.* **255**, 131-139.
- Demir, N., Basaranoglu, M., Huyut, Z., Deger, I., Karaman, K., Sekeroglu, M. R. and Tuncer, O. (2017). The relationship between mother and infant plasma trace element and heavy metal levels and the risk of neural tube defect in infants. *J. Matern. Fetal. Neonatal. Med.* **1-8**.
- Dey, A. C., Shahidullah, M., Mannan, M. A., Noor, M. K., Saha, L. and Rahman, S. A. (2010). Maternal and neonatal serum zinc level and its relationship with neural tube defects. *J. Health Popul. Nutr.* **28**, 343-350.
- Duan, J. and Nilsson, L. (2006). Effect of Zn²⁺ on DNA recognition and stability of the p53 DNA-binding domain. *Biochemistry* **45**, 7483-7492.
- Dufner-Beattie, J., Huang, Z. L., Geiser, J., Xu, W. and Andrews, G. K. (2006). Mouse ZIP1 and ZIP3 genes together are essential for adaptation to dietary zinc deficiency during pregnancy. *Genesis* **44**, 239-251.
- el-Deiry, W. S., Tokino, T., Velculescu, V. E., Levy, D. B., Parsons, R., Trent, J. M., Lin, D., Mercer, W. E., Kinzler, K. W. and Vogelstein, B. (1993). WAF1, a potential mediator of p53 tumor suppression. *Cell* **75**, 817-825.
- Erhardt, P., Tomaselli, K. J. and Cooper, G. M. (1997). Identification of the MDM2 oncoprotein as a substrate for CPP32-like apoptotic proteases. *J. Biol. Chem.* **272**, 15049-15052.
- Esser, C., Scheffner, M. and Höfheld, J. (2005). The chaperone-associated ubiquitin ligase CHIP is able to target p53 for proteasomal degradation. *J. Biol. Chem.* **280**, 27443-27448.
- Fang, S., Jensen, J. P., Ludwig, R. L., Vousden, K. H. and Weissman, A. M. (2000). Mdm2 is a RING finger-dependent ubiquitin protein ligase for itself and p53. *J. Biol. Chem.* **275**, 8945-8951.
- Force, U. S. P. S. T., Bibbins-Domingo, K., Grossman, D. C., Curry, S. J., Davidson, K. W., Epling, J. W. Jr., Garcia, F. A., Kemper, A. R., Krist, A. H., Kurth, A. E. et al. (2017). Folic acid supplementation for the prevention of neural tube defects: US preventive services task force recommendation statement. *JAMA* **317**, 183-189.
- Galea, G. L., Cho, Y. J., Galea, G., Mole, M. A., Rolo, A., Savery, D., Moulding, D., Culshaw, L. H., Nikolopoulou, E., Greene, N. D. E. et al. (2017). Biomechanical coupling facilitates spinal neural tube closure in mouse embryos. *Proc. Natl. Acad. Sci. USA* **114**, E5177-E5182.
- Gao, H.-L., Zheng, W., Xin, N., Chi, Z.-H., Wang, Z.-Y., Chen, J. and Wang, Z.-Y. (2009). Zinc deficiency reduces neurogenesis accompanied by neuronal apoptosis through caspase-dependent and -independent signaling pathways. *Neurotox. Res.* **16**, 416-425.
- Gao, H., Zhao, L., Wang, H., Xie, E., Wang, X., Wu, Q., Yu, Y., He, X., Ji, H., Rink, L. et al. (2017). Metal transporter Slc39a10 regulates susceptibility to inflammatory stimuli by controlling macrophage survival. *Proc. Natl. Acad. Sci. USA* **114**, 12940-12945.
- Geyer, R. K., Yu, Z. K. and Maki, C. G. (2000). The MDM2 RING-finger domain is required to promote p53 nuclear export. *Nat. Cell Biol.* **2**, 569-573.
- Golalipour, M. J., Vakili, M. A., Mansourian, A. R. and Mobasheri, E. (2009). Maternal serum zinc deficiency in cases of neural tube defect in Gorgan, north Islamic Republic of Iran. *East Mediterr Health J.* **15**, 337-344.
- Gower-Winter, S. D., Corniola, R. S., Morgan, T. J. Jr. and Levenson, C. W. (2013). Zinc deficiency regulates hippocampal gene expression and impairs neuronal differentiation. *Nutr. Neurosci.* **16**, 174-182.
- Greene, N. D. E., Stanier, P. and Copp, A. J. (2009). Genetics of human neural tube defects. *Hum. Mol. Genet.* **18**, R113-R129.
- Greene, N. D., Leung, K.-Y., Gay, V., Burren, K., Mills, K., Chitty, L. S. and Copp, A. J. (2016). Inositol for the prevention of neural tube defects: a pilot randomised controlled trial. *Br. J. Nutr.* **115**, 974-983.
- Groenen, P. M., Peer, P. G., Wevers, R. A., Swinkels, D. W., Franke, B., Mariman, E. C. and Steegers-Theunissen, R. P. (2003). Maternal myo-inositol, glucose, and zinc status is associated with the risk of offspring with spina bifida. *Am. J. Obstet. Gynecol.* **189**, 1713-1719.
- Harding, A. J., Dreosti, I. E. and Tulsi, R. S. (1988). Zinc deficiency in the 11 day rat embryo: a scanning and transmission electron microscope study. *Life Sci.* **42**, 889-896.

- Haupt, Y., Maya, R., Kazaz, A. and Oren, M. (1997). Mdm2 promotes the rapid degradation of p53. *Nature* **387**, 296-299.
- Hinks, L. J., Ogilvy-Stuart, A., Hambidge, K. M. and Walker, V. (1989). Maternal zinc and selenium status in pregnancies with a neural tube defect or elevated plasma alpha-fetoprotein. *Br J Obstet Gynaecol* **96**, 61-66.
- Hojyo, S. and Fukada, T. (2016). Zinc transporters and signaling in physiology and pathogenesis. *Arch Biochem Biophys* **611**, 43-50.
- Hurley, L. S. (1969). Zinc deficiency in the developing rat. *Am. J. Clin. Nutr.* **22**, 1332-1339.
- Jin, J. (2017). Folic acid supplementation for prevention of neural tube defects. *JAMA* **317**, 222.
- Kim, T.-H., Goodman, J., Anderson, K. V. and Niswander, L. (2007). Phactr4 regulates neural tube and optic fissure closure by controlling PP1-, Rb-, and E2F1-regulated cell-cycle progression. *Dev. Cell* **13**, 87-102.
- Komarov, P. G., Komarova, E. A., Kondratov, R. V., Christov-Tselkov, K., Coon, J. S., Chernov, M. V. and Gudkov, A. V. (1999). A chemical inhibitor of p53 that protects mice from the side effects of cancer therapy. *Science* **285**, 1733-1737.
- Kussie, P. H., Gorina, S., Marechal, V., Elenbaas, B., Moreau, J., Levine, A. J. and Pavletich, N. P. (1996). Structure of the MDM2 oncoprotein bound to the p53 tumor suppressor transactivation domain. *Science* **274**, 948-953.
- Leger, A. S., Elwood, P. C. and Morton, M. S. (1980). Neural tube malformations and trace elements in water. *J. Epidemiol. Community Health* **34**, 186-187.
- Leung, K.-Y., Pai, Y. J., Chen, Q., Santos, C., Calvani, E., Sudiwala, S., Savery, D., Ralsler, M., Gross, S. S., Copp, A. J. et al. (2017). Partitioning of one-carbon units in folate and methionine metabolism is essential for neural tube closure. *Cell Rep.* **21**, 1795-1808.
- Li, M., Chen, D., Shiloh, A., Luo, J., Nikolaev, A. Y., Qin, J. and Gu, W. (2002). Deubiquitination of p53 by HAUSP is an important pathway for p53 stabilization. *Nature* **416**, 648-653.
- Li, M., Brooks, C. L., Wu-Baer, F., Chen, D., Baer, R. and Gu, W. (2003). Mono- versus polyubiquitination: differential control of p53 fate by Mdm2. *Science* **302**, 1972-1975.
- Li, H., Zhang, J., Chen, S., Wang, F., Zhang, T. and Niswander, L. (2018). Genetic contribution of retinoid-related genes to neural tube defects. *Hum. Mutat.* **39**, 550-562.
- Livingstone, L. R., White, A., Sprouse, J., Livanos, E., Jacks, T. and Tlsty, T. D. (1992). Altered cell cycle arrest and gene amplification potential accompany loss of wild-type p53. *Cell* **70**, 923-935.
- Ma, J., Martin, J. D., Xue, Y., Lor, L. A., Kennedy-Wilson, K. M., Sinnamon, R. H., Ho, T. F., Zhang, G., Schwartz, B., Tummino, P. J. et al. (2010). C-terminal region of USP7/HAUSP is critical for deubiquitination activity and contains a second mdm2/p53 binding site. *Arch. Biochem. Biophys.* **503**, 207-212.
- Marchenko, N. D. and Moll, U. M. (2007). The role of ubiquitination in the direct mitochondrial death program of p53. *Cell Cycle* **6**, 1718-1723.
- Massarwa, R. and Niswander, L. (2013). In toto live imaging of mouse morphogenesis and new insights into neural tube closure. *Development* **140**, 226-236.
- Mihara, M., Erster, S., Zaika, A., Petrenko, O., Chittenden, T., Pancoska, P. and Moll, U. M. (2003). p53 has a direct apoptogenic role at the mitochondria. *Mol. Cell* **11**, 577-590.
- Morris, D. R. and Levenson, C. W. (2013). Zinc regulation of transcriptional activity during retinoic acid-induced neuronal differentiation. *J. Nutr. Biochem.* **24**, 1940-1944.
- Nomura, K., Klejnot, M., Kowalczyk, D., Hock, A. K., Sibbet, G. J., Vousden, K. H. and Huang, D. T. (2017). Structural analysis of MDM2 RING separates degradation from regulation of p53 transcription activity. *Nat. Struct. Mol. Biol.* **24**, 578-587.
- Nuttall, J. R., Supasai, S., Kha, J., Vaeth, B. M., Mackenzie, G. G., Adamo, A. M. and Oteiza, P. I. (2015). Gestational marginal zinc deficiency impaired fetal neural progenitor cell proliferation by disrupting the ERK1/2 signaling pathway. *J. Nutr. Biochem.* **26**, 1116-1123.
- Pfaender, S., Föhr, K., Lutz, A.-K., Putz, S., Achberger, K., Linta, L., Liebau, S., Boeckers, T. M. and Grabrucker, A. M. (2016). Cellular zinc homeostasis contributes to neuronal differentiation in human induced pluripotent stem cells. *Neural Plast.* **2016**, 3760702.
- Pochampally, R., Fodera, B., Chen, L., Shao, W., Levine, E. A. and Chen, J. (1998). A 60 kd MDM2 isoform is produced by caspase cleavage in non-apoptotic tumor cells. *Oncogene* **17**, 2629-2636.
- Pyrgaki, C., Trainor, P., Hadjantonakis, A.-K. and Niswander, L. (2010). Dynamic imaging of mammalian neural tube closure. *Dev. Biol.* **344**, 941-947.
- Ra, H., Kim, H.-L., Lee, H.-W. and Kim, Y.-H. (2009). Essential role of p53 in TPEN-induced neuronal apoptosis. *FEBS Lett.* **583**, 1516-1520.
- Ray, H. J. and Niswander, L. A. (2016). Dynamic behaviors of the non-neural ectoderm during mammalian cranial neural tube closure. *Dev. Biol.* **416**, 279-285.
- Rayman, J. B., Karl, K. A. and Kandel, E. R. (2018). TIA-1 self-multimerization, phase separation, and recruitment into stress granules are dynamically regulated by Zn(2). *Cell Rep.* **22**, 59-71.
- Rhee, J. M., Pirity, M. K., Lackan, C. S., Long, J. Z., Kondoh, G., Takeda, J. and Hadjantonakis, A.-K. (2006). In vivo imaging and differential localization of lipid-modified GFP-variant fusions in embryonic stem cells and mice. *Genesis* **44**, 202-218.
- Schlett, K. and Madarasz, E. (1997). Retinoic acid induced neural differentiation in a neuroectodermal cell line immortalized by p53 deficiency. *J. Neurosci. Res.* **47**, 405-415.
- Sekihara, K., Harashima, N., Tongu, M., Tamaki, Y., Uchida, N., Inomata, T. and Harada, M. (2013). Pifithrin-mu, an inhibitor of heat-shock protein 70, can increase the antitumor effects of hyperthermia against human prostate cancer cells. *PLoS ONE* **8**, e78772.
- Seth, R., Corniola, R. S., Gower-Winter, S. D., Morgan, T. J., Jr., Bishop, B. and Levenson, C. W. (2015). Zinc deficiency induces apoptosis via mitochondrial p53- and caspase-dependent pathways in human neuronal precursor cells. *J. Trace Elem. Med. Biol.* **30**, 59-65.
- Shloush, J., Vlassov, J. E., Engson, I., Duan, S., Saridakis, V., Dhe-Paganon, S., Raught, B., Sheng, Y. and Arrowsmith, C. H. (2011). Structural and functional comparison of the RING domains of two p53 E3 ligases, Mdm2 and Pirh2. *J. Biol. Chem.* **286**, 4796-4808.
- Sohn, D., Graupner, V., Neise, D., Essmann, F., Schulze-Osthoff, K. and Janicke, R. U. (2009). Pifithrin-alpha protects against DNA damage-induced apoptosis downstream of mitochondria independent of p53. *Cell Death Differ.* **16**, 869-878.
- Srinivas, M., Gupta, D. K., Rathi, S. S., Grover, J. K., Vats, V., Sharma, J. D. and Mitra, D. K. (2001). Association between lower hair zinc levels and neural tube defects. *Indian J. Pediatr.* **68**, 519-522.
- Strand, O. A., Aziz, G., Ali, S. F., Paulsen, R. E., Hansen, T. V. and Rongved, P. (2013). Synthesis and initial in vitro biological evaluation of two new zinc-chelating compounds: comparison with TPEN and PAC-1. *Bioorg. Med. Chem.* **21**, 5175-5181.
- Strom, E., Sathe, S., Komarov, P. G., Chernova, O. B., Pavlovskaya, I., Shyshynova, I., Bosykh, D. A., Burdelya, L. G., Macklis, R. M., Skaliter, R. et al. (2006). Small-molecule inhibitor of p53 binding to mitochondria protects mice from gamma radiation. *Nat. Chem. Biol.* **2**, 474-479.
- Szewczyk, B. (2013). Zinc homeostasis and neurodegenerative disorders. *Front Aging Neurosci.* **5**, 33.
- Toledo, F. and Wahl, G. M. (2006). Regulating the p53 pathway: in vitro hypotheses, in vivo veritas. *Nat. Rev. Cancer* **6**, 909-923.
- Tropepe, V., Sibilina, M., Ciruna, B. G., Rossant, J., Wagner, E. F. and van der Kooy, D. (1999). Distinct neural stem cells proliferate in response to EGF and FGF in the developing mouse telencephalon. *Dev. Biol.* **208**, 166-188.
- Vaseva, A. V. and Moll, U. M. (2009). The mitochondrial p53 pathway. *Biochim. Biophys. Acta* **1787**, 414-420.
- Velie, E. M., Block, G., Shaw, G. M., Samuels, S. J., Schaffer, D. M. and Kulldorff, M. (1999). Maternal supplemental and dietary zinc intake and the occurrence of neural tube defects in California. *Am. J. Epidemiol.* **150**, 605-616.
- Viswanathan, M., Treiman, K. A., Kish-Doto, J., Middleton, J. C., Coker-Schwimmer, E. J. and Nicholson, W. K. (2017). Folic acid supplementation for the prevention of neural tube defects: an updated evidence report and systematic review for the US preventive services task force. *JAMA* **317**, 190-203.
- Wallingford, J. B., Niswander, L. A., Shaw, G. M. and Finnell, R. H. (2013). The continuing challenge of understanding, preventing, and treating neural tube defects. *Science* **339**, 1222002.
- Wang, F. D., Bian, W., Kong, L. W., Zhao, F. J., Guo, J. S. and Jing, N. H. (2001). Maternal zinc deficiency impairs brain nestin expression in prenatal and postnatal mice. *Cell Res.* **11**, 135-141.
- Wilde, J. J., Petersen, J. R. and Niswander, L. (2014). Genetic, epigenetic, and environmental contributions to neural tube closure. *Annu. Rev. Genet.* **48**, 583-611.
- Yan, L., Wang, B., Li, Z., Liu, Y., Huo, W., Wang, J., Li, Z. and Ren, A. (2017). Association of essential trace metals in maternal hair with the risk of neural tube defects in offspring. *Birth Defects Res.* **109**, 234-243.
- Zeyrek, D., Soran, M., Cakmak, A., Kocyigit, A. and Iscan, A. (2009). Serum copper and zinc levels in mothers and cord blood of their newborn infants with neural tube defects: a case-control study. *Indian Pediatr.* **46**, 675-680.
- Zimmerman, A. W. and Rowe, D. W. (1983). Cellular zinc accumulation in anencephaly and spina bifida. *Z Kinderchir* **38** Suppl. 2, 65-67.